Author Manuscript

Author Manuscript

Author Manuscript

Author Manuscript

HHS Public Access

Author manuscript

Clin Neurophysiol. Author manuscript; available in PMC 2019 June 13.

Published in final edited form as:

Clin Neurophysiol. 2018 September ; 129(9): 1873–1883. doi:10.1016/j.clinph.2018.04.749.

Impact of non-brain anatomy and coil orientation on inter- and intra-subject variability in TMS at midline

Erik G. Lee[a,b,*], **Priyam Rastogi**[b], **Ravi L. Hadimani**[c,b], **David C. Jiles**[b], and **Joan A. Camprodon**[a]

[a] Laboratory for Neuropsychiatry and Neuromodulation, Department of Psychiatry, Massachusetts General Hospital, Harvard Medical School, 149 13th Street, Boston, Massachusetts 02129, USA

[b] Department of Electrical and Computer Engineering, Iowa State University, 2520 Osborne Drive, Ames, Iowa 50011, USA

[c] Department of Mechanical and Nuclear Engineering, Virginia Commonwealth University, 401 West Main Street, Richmond, Virginia 23284, USA

Abstract

Objective—To investigate inter-subject variability with respect to cerebrospinal fluid thickness and brain-scalp distance, and to investigate intra-subject variability with different coil orientations.

Methods—Simulations of the induced electric field (E-Field) using a figure-8 coil over the vertex were conducted on 50 unique head models and varying orientations on 25 models. Metrics exploring stimulation intensity, spread, and localization were used to describe inter-subject variability and effects of non-brain anatomy.

Results—Both brain-scalp distance and CSF thickness were correlated with weaker stimulation intensity and greater spread. Coil rotations show that for the dorsal portion of the stimulated brain, E-Field intensities are highest when the anterior-posterior axis of the coil is perpendicular to the longitudinal fissure, but highest for the medial portion of the stimulated brain when the coil is oriented parallel to the longitudinal fissure.

Conclusions—Normal anatomical variation in healthy individuals leads to significant differences in the site of TMS, the intensity, and the spread. These variables are generally neglected but could explain significant variability in basic and clinical studies.

Significance—This is the first work to show how brain-scalp distance and cerebrospinal fluid thickness influence focality, and to show the disassociation between dorsal and medial TMS.

[*]Corresponding author at: Laboratory for Neuropsychiatry and Neuromodulation, Department of Psychiatry, Massachusetts General Hospital, Harvard Medical School, 149 13th Street, Boston, Massachusetts 02129, USA. erik.lee.mn@gmail.com (E.G. Lee).

Conflicts of interest

The authors have no conflicts of interest to state.

Appendix A. Supplementary data

Supplementary data associated with this article can be found, in the online version, at https://doi.org/10.1016/j.clinph.2018.04.749.

Author Manuscript Author Manuscript Author Manuscript Author Manuscript

Keywords

TMS; Inter-subject variability; Cerebrospinal fluid; Focality; Orientation; Lower-limb

1. Introduction

Transcranial magnetic stimulation (TMS) is an established neuromodulation technology that utilizes strong, transient magnetic fields generated by an electromagnetic coil placed on the scalp to induce electric fields in underlying brain tissues (Barker et al., 1985; Walsh and Cowey, 2000; Pascual-Leone et al., 1994; Berlim et al., 2014). The strength and distribution of the time-varying magnetic fields are dependent on both the geometry and the amount of current traveling through the TMS coil (Deng et al. 2013; Rastogi et al., 2017; Zangen et al., 2005; Thielscher and Kammer, 2004). Beyond coil architecture and pulse intensity, the induced electric field is also dependent on fixed variables unique to individuals such as the geometry and electrical properties of anatomies in and around the brain (Lee et al., 2016; Thielscher et al., 2011; Opitz et al., 2011; Stokes et al., 2013; Janssen et al., 2015; Laakso et al., 2014; Miranda et al., 2003).

Computer simulations utilizing heterogeneous tissue conductivities and finite element physics solvers provide a framework for understanding how anatomy shapes stimulation and contributes to inter-subject variability. Until recently, most TMS modeling studies relied on greatly simplified head models (spherical or homogenous) or one or two heterogeneous head models (Deng et al. 2013; Bijsterbosch et al., 2012; Janssen et al., 2015). These simulations allowed researchers to look at how both coils and anatomy influence stimulation within individuals, but were limited in their ability to show how stimulation varies between individuals. Recent developments in modeling tools have improved the generation of heterogeneous head models (Windhoff et al., 2013; Thielscher et al., 2015), facilitating the use of several models in studies (Krieg et al., 2015; Lee et al., 2016; Opitz et al., 2013; Laakso et al., 2016a, 2016b; Opitz et al., 2016; Bungert et al., 2016). This is important because the induced E-Field in a single head cannot be representative of the induced E-Field for a population, given the significant differences in head anatomy. Through simulations on larger groups of head models, it is possible to model more accurate and generalizable distributions of common E-Field profiles, and to quantify the contribution of anatomical differences to stimulation effects.

In our recent work we studied the relationship between brain-scalp distance (BSD) and TMS stimulation intensity in 50 head models of healthy subjects from the Human Connectome Project (HCP) database, and quantified the significant negative correlation between BSD and maximum stimulation intensity (Lee et al., 2016). Additionally, we hypothesized that BSD was related to stimulation focality, but no statistically significant relationship was observed. The current paper aims to build on the work of our previous study, using the same 50 head models but applying new and more sophisticated analyses aiming to further understand and quantify the impact of individual head anatomy and coil orientation on TMS effects. Specifically, we aim to characterize the inter-subject variability in the TMS-induced electric field defined by the stimulation location (point of maximum stimulation), intensity (E-max)

Author Manuscript Author Manuscript Author Manuscript Author Manuscript

and spread (V-Half and A-Half), and critically, examine how these differences are explained by the normal variation in two non-brain anatomy variables: BSD and CSF thickness. In addition to studying the impact of (fixed) anatomical variables, we further characterize the impact of coil orientation on the electric field intensity and distribution.

Beyond new aims and hypotheses, important methodological differences between this work and our previous work include the incorporation of additional thresholding techniques to assess both stimulation intensity and spread. With these new thresholds, a clear contribution of BSD to stimulation focality emerges. Further, previously unexplored differences in local cerebrospinal fluid (CSF) thickness between individuals are evaluated to understand how this highly conductive fluid shapes stimulation.

Modeling varying coil orientations, we also assess the ideal position for stimulation of bilateral midline structures. Previous studies show a clear relationship between stimulation intensity over the hand motor area and coil orientation, providing evidence that stimulation is optimized when the anterior-posterior axis of the coil is oriented perpendicular to the precentral gyrus (Opitz et al., 2011; Laakso et al., 2014). Similarly, simulation results from Janssen et al. (Janssen et al., 2015) showed in a single model a preference for the coil to be oriented perpendicular to the longitudinal fissure over the supplementary motor area (SMA). It would be expected that this relationship applies to any midline target, including the vertex, but these results have yet to be confirmed, particularly in a greater number of subjects. More importantly, whether the effects of coil orientation are equivalent over dorsal and medial midline structures has yet to be studied. This is of practical relevance as a number of TMS applications aim at targets along the longitudinal fissure, such as the motor cortex (Chieffo et al., 2014; Kakuda et al., 2013; Pulvermuller et al., 2005) and the supplementary motor area (Verwey et al., 2002; Cunnington et al., 1996; Oliveri et al., 2003) in motor neurophysiology, the pre-supplementary motor area (Kennerley, 2003; Mantovani et al., 2010; Obeso et al., 2013; Rochas et al., 2013) in obsessive compulsive disorder and behavioral inhibition, and the dorsomedial prefrontal cortex (Downar et al., 2014; Salomons et al., 2013) in depression and mood disorders.

The results presented in this paper highlight how unique, yet normal, anatomical features can affect both stimulation intensity and spread, and how coil orientation can be used to preferentially target dorsal or medial midline structures. Understanding the influence that anatomical factors have on the site, intensity and spread of stimulation is critical to explain the variability in the physiological, behavioral and clinical effects of TMS. This knowledge could translate into methodological improvements aiming to normalize stimulation parameters and maximize treatment outcomes.

2. Methods

2.1. Model development

For this study, 50 finite element models were developed from Human Connectome Project participants' MRI images (Van Essen et al., 2012) using the automated SimNIBS pipeline (Windhoff et al., 2013). All models consist of meshes for skin, skull, CSF, grey matter, white matter, cerebellum, and ventricles. The set of 50 models is representative of young, healthy

Author Manuscript Author Manuscript Author Manuscript Author Manuscript

adults age 22–35 years. In total, there were 25 male models and 25 female models. A detailed description of the model generation protocol can be found in the Supplementary Methods and Results.

2.2. Simulations

Finite element simulations were conducted in SEMCAD X (SEMCAD, 2014) on all 50 head models to calculate the induced electric field from TMS. In all simulations, a Magstim 70 mm Figure-8 coil was modeled as the stimulating coil. The Magstim 70 mm Figure-8 coil was chosen for stimulation due to its popularity in research studies (Grunhaus et al., 2003; Kleim et al., 2006; Maeda et al., 2000). The current source for the coil was simulated as a 5000 A, 2500 Hz sinusoidal wave, which is comparable in intensity to a common value of a stimulator's maximum output (Hovey and Jalinous, 2006; Crowther et al., 2014).

The main set of simulations used in this study were carried out with 1 mm isotropic voxels. Each voxel was assigned to a specific segmented anatomy and then assigned an isotropic electrical conductivity and relative permittivity for the frequency used in the simulations (2500 Hz) based on a standard set of previously published values, seen in Supplementary Table 1 (Hasgall et al., 2012). A supplementary set of simulations were also conducted with 0.5 mm isotropic voxels to test the stability of simulation results. For these simulations, two models with thin CSF and two models with thick CSF were chosen. A comparison between these four models' simulations at 0.5 mm vs. 1 mm voxels can be seen in the Supplementary Methods and Results, along with more indepth technical details behind other aspects of simulation setup.

In the main set of simulations used in this study, two groupings of simulations will be presented. The first grouping of simulations were conducted on 50 head models with the coil placed tangential to the surface of the scalp over the vertex, with the coil handle running posterior to anterior as seen in Fig. 1. The direction of the current traveling through the coil is irrelevant for the analyses being conducted, as only the magnitude of the induced electric field will be taken into account, which is not affected by current polarity. Although the target of stimulation was chosen with reference to non-brain landmarks, the vertex has been used commonly in neurophysiology studies for identification of the medial portion of the motor cortex and thus the lower-limb motor area (Sakai et al., 1994; Priori et al., 1993).

The second set of simulations include 225 cumulative placements on a random subset of 25 of the 50 models, to explore the effects of coil orientation. The center of the coil remained in the same location over the vertex for all orientations, but the coil was rotated in 20° increments from 0° to 160° so that all possible orientations of the coil were considered. This range covers all orientations because rotations from 180–340° will have an identical E-Field magnitude as 0–160° due to the symmetry of the coil. In later figures, the 0° orientation was also visualized as the 180° orientation for symmetry.

2.3. Post processing

Several metrics were calculated through post-processing with custom Matlab scripts. The first two metrics include brain-scalp distance (BSD) and CSF thickness at the site of stimulation. To calculate BSD, all voxels superior of the brain that are identified as air and

Author Manuscript Author Manuscript Author Manuscript Author Manuscript

border skin are first collected. Then all border voxels that are contained within a 2 cm radius cylinder drawn around the vertex are selected. For each voxel in this group, the minimum Euclidian distance to the closest brain voxel was calculated, and the mean distance of all voxels was taken as the value for BSD. For CSF thickness the same process was taken, only instead of air voxels that border skin being used to calculate distance, skull voxels that border CSF were used to calculate distance.

Next, three additional metrics were designed including E-Max, V-Half, and A-Half. First, E-Max is defined as the maximum electric field intensity in the brain for a given simulation. This was used in our previous work (Lee et al., 2016), and was taken from the single voxel in the brain with the largest electric field intensity. Research from Laakso et al. (Laakso and Hirata, 2012) and Thielscher et al. (Thielscher et al., 2011) has shown how finite element simulations with cubic voxels may be sensitive to the voxel stair-casing error, which can create numerical artifacts in voxels at the interface of tissues with large differences in conductivity, such as CSF and grey matter. Because the E-Field intensity in a single voxel may not be a robust measure, E-Max was chosen to be calculated at a few different thresholds including 1 mm^3, 10 mm^3, 100 mm^3, and 1 cm^3. In all thresholds, the value of E-Max was calculated as the mean E-Field intensity of the top 1, 10, 100, or 1000, 1 mm^3 voxels in the brain.

These different E-Max thresholds were then taken to calculate V-Half and A-Half which are measures representative of the total brain volume receiving stimulation, and the surface area of the brain receiving stimulation, respectively. V-Half is then defined as the volume of the brain in a simulation with an E-Field intensity greater than at least half of E-Max. A-Half is the same except the voxels that are counted towards the area receiving stimulation are limited to grey matter voxels that are bordering CSF. Because the A-Half results were very similar to V-Half, the A-Half results and discussion have been moved to the Supplementary Methods and Results.

The described metrics were all calculated using the four different E-Max thresholds (1 mm^3, 10 mm^3, 100 mm^3, and 1 cm^3) to explore the relationships between mentioned stimulation variables and both BSD and local CSF thickness at the site of stimulation. It should be mentioned that these stimulation thresholds are defined arbitrarily. Although they are representative of how the induced electric field from TMS is distributed throughout the brain, using half of E-Max to define surface stimulation (A-Half), and volume stimulation (V-Half) may not be accurately representative of the neuronal population caused to depolarize from TMS. Instead, these thresholds are simply a way of normalizing stimulation intensities between individuals so we can assess stimulation spread, just as every participant in most TMS studies receives unique doses normalized to their motor threshold.

To also evaluate the stability of these thresholds, the four high-resolution simulations mentioned in the **Simulations** section were used to recalculate E-Max and V-Half. The results of these simulations show that the E-Max and V-Half 1 cm^3 thresholds are particularly reliable at different voxel resolutions. The E-Max and V-Half 1 mm^3 thresholds, which are based off of the electric field intensity of the single voxel receiving the greatest stimulation intensity, showed acceptable levels of reproducibility for three of the four

Author Manuscript Author Manuscript Author Manuscript Author Manuscript

models, and weak reproducibility for one model (see Supplementary Methods and Results for more details). Because of these differences in reproducibility, and because the 1 cm^3 thresholds are more strongly tied to BSD and CSF thickness (as seen later in Results), the 1 cm^3 results will be the main focus of the paper. More detailed results based off of the other thresholding schemes can still be seen in the Supplementary Methods and Results.

The next calculated metrics used for the main set of simulations were used to localize the region of the brain receiving the strongest E-Field intensity. As with the previous metrics described, this was calculated using multiple scales. The first calculation simply took the location in the brain with the highest E-Field intensity for each simulation. The second calculation involved drawing 8 mm diameter spheres around voxels with peak E-Field intensities, and selecting the location with the greatest mean intensity throughout the sphere (voxels restricted to grey matter and white matter). If all voxels neighboring a point were contained within the brain, then the maximum number of voxels used to calculate the mean intensity would be 257. The voxel with the largest mean intensity using this measure was then chosen as the location of maximum stimulation for the spherical metric.

Similarly, four 5 mm diameter spheres were placed in the brain for each model that was used in the coil rotation simulations (see Fig. 2 for example placement). The goal of these manually placed seeds was to determine if coil orientation had differential effects depending on the relative target of stimulation. The first seed was placed in the left hemisphere roughly 1.5 cm lateral of the most superior and midline section of the brain directly beneath the coil, where then the second seed is then placed. The third seed is roughly 1 cm inferior of the most superior midline section (seed 2), and the fourth seed is roughly another 1 cm more inferior. The sagittal center of each seed was placed within 2 mm of the sagittal center of the coil. Within this +/−2 mm range, the slice was chosen where the anatomical seed placement using the described positioning guidelines for the four seeds could be most similar to the example seen in Fig. 2. The reason for allowing this range is because some models did not have clear anatomical targets at the most center sagittal slice due to CSF filled sulci or gaps in brain continuity. In cases where multiple slices provided similar targets, the slice closest to the sagittal center of the coil was used.

For statistical inference, Pearson correlation coefficients between anatomical and stimulation metrics were computed. Further, in a supplementary step for assessing the relationship between CSF and both E-Max and V-Half, the effects of BSD on E-Max and V-Half were linearly regressed before computation of correlation coefficients to test whether or not CSF had a unique role in determining the site of stimulation, rather than only being important due to its contribution to BSD. For all relationships, Pearson correlation coefficients were converted to p-values using two-tailed t-tests. To test sex differences in E-Max and V-Half, unpaired two-tailed t-tests were utilized. Findings were considered statistically significant for all probabilities satisfying $p < 0.05$. To also directly compare the predictive power of BSD and CSF thickness, two-tailed t-tests were ran in the cocor package (Diedenhofen and Musch, 2015), based on the test from Williams (Williams, 1959). Throughout the presentation of results, no forms of multiple comparisons corrections were employed.

Author Manuscript Author Manuscript Author Manuscript Author Manuscript

3. Results

3.1. General variability in E-Max and V-Half

Analysis of simulation results shows that in our random cohort of 50 healthy subjects, the individual receiving the weakest stimulation intensity, defined by E-Max (1 cm^3), will receive 83 Volts/meter (V/m). In comparison, the individual receiving the strongest stimulation intensity will receive 188 V/m (227% higher). To illustrate this difference, if both subjects only need for example, 100 V/m for the appropriate stimulation response, and the TMS stimulator has a max output of 5000 Amps, then the first subject with the lowest E-Max (1 cm^3) will need a dose of 122% MSO (which would be above the maximum output of the device), while the second subject with the high E-Max (1 cm^3) will need a dose of 53% MSO.

Extending this illustration, if the stimulation intensity is scaled so all subjects receive 100 V/m at the maximum location, by using the E-Max (1 cm^3) metric, we can use V-Half (1 cm^3) to understand how much brain volume is stimulated at a minimum of 50 V/m (an arbitrary threshold for illustration purposes). This shows that the subject with the lowest V-Half (1 cm^3), and thus the smallest volume of brain receiving stimulation, will only have 6.8 cm^3 receiving stimulation at or above 50 V/m. In contrast, the subject with the largest brain volume receiving stimulation will have 24.4 cm^3 of their brain receiving stimulation.

Histograms of the distribution of both E-Max (1 cm^3) and V-Half (1 cm^3) can be seen in Fig. 3. Further, figures exploring the volume of the brain stimulated above several absolute thresholds (50, 75, 100, and 125 V/m), and a detailed discussion of the distribution of anatomical variability can be seen in the Supplementary Methods and Results.

3.2. Brain-Scalp distance with E-Max and V-Half

As shown in our previous work (Lee et al., 2016) a strong relationship was observed between E-Max (1 mm^3) and BSD ($r = -0.74$, $p < 0.001$, t-score = −7.62), such that greater BSDs lead to weaker stimulation intensities. The relationship between BSD and E-Max is strong with all thresholds, starting at 1 mm^3, but grows as the threshold becomes larger up to E-Max (1 cm^3) ($r = -0.85$, $p < 0.001$, t-score = −11.18) (see Fig. 4(a)). It is important to note that with a threshold of 1 cm^3, BSD explains 72% of the variability in E-Max across subjects, but 28% of that variance is accounted by other factors.

Using the less reliable V-Half (1 mm^3) metric, there is no statistically significant relationship observed with BSD ($r = 0.22$, $p = 0.13$, t-score = 1.56). Seen in Fig. 4(c) though, using the more reliable V-Half (1 cm^3), a notable relationship emerges between V-Half (1 cm^3) and BSD ($r = 0.40$, $p = 0.004$, t-score = 3.02), such that greater BSDs lead to a larger volume of the brain receiving stimulation. This outcome with more reliable thresholding techniques is consistent with our previous results on simplified head models (Lee et al., 2016), which again were not reproduced in our set of simulations on 50 heterogeneous models with a metric comparable to V-Half (1 mm^3), only scaled to total brain volume.

Author Manuscript Author Manuscript Author Manuscript Author Manuscript

3.3. Cerebrospinal fluid thickness with E-Max and V-Half

Beyond BSD, results show that CSF thickness is a significant predictor of both E-Max and V-Half. Shown in Fig. 4(c and d), thicker CSF leads to both weaker stimulation intensities and a larger proportion of the brain receiving stimulation. For CSF thickness, this trend is statistically significant ($p < 0.001$) for all forms of thresholding (1 mm^3 to 1 cm^3) for both E-Max and V-Half. In our results, BSD was shown to be a greater predictor of stimulation intensity, and CSF thickness a greater predictor of stimulation spread. Making a direct comparison to test whether or not these differences in predictive power are statistically significant, we see that, as expected, BSD is a greater predictor of E-Max (1 cm^3) ($p = 0.002$, $t = -3.24$, Williams' t). Although we observed a notable difference in the predictive power of CSF over BSD for V-Half (1 cm^3) ($r = 0.40$, $r = 0.60$ respectively), a direct comparison shows that this difference is not statistically significant ($p = 0.12$, $t = 1.57$, Williams' t).

It could be expected that the effects of CSF thickness are only present because CSF thickness contributes to overall BSD. To address this confounding concern, we tested the relationship between CSF thickness and both E-Max and V-Half controlling for BSD in a linear regression (Fig. 4(e and f)). These results confirm that there is still a significant relationship between CSF thickness and both E-Max and V-Half after regressing out the overall effect of brain scalp distance. Further, using both BSD and CSF thickness to account for E-Max (1 cm^3), the stepwise linear model now explains 80% of the variability in E-Max (opposed to 72% for BSD alone). For V-Half (1 cm^3) similarly, the full model with BSD and CSF thickness explains 36% of the variability (opposed to 15% for BSD alone).

3.4. Location of maximum stimulation

Results from both using a single voxel, and using a 8 mm diameter sphere to highlight the location in the brain receiving the highest stimulation intensities yielded similar results as seen in Fig. 5. This figure highlights in an axial plane, the extent to which the location of maximum stimulation corresponds to the expected "hot spot" beneath the center of the coil. It is shown that the location of maximum stimulation spans 4 cm in the anterior/posterior direction and 3 cm in the left/right direction. It should be noted that some of the left/right variation may be emphasized by the longitudinal fissure which runs along the sagital plane.

When the distance from the location of maximum stimulation to the expected "hot spot" (directly beneath the coil center) is calculated, this measure is shown to be unrelated to brain-scalp distance BSD ($p = 0.95$), but significantly related to CSF thickness ($r = 0.32$, $p = 0.023$, t-score = 2.34). This corresponds to what was observed in the analysis of both V-Half and A-Half, where thicker layers of CSF were related to an increase in the overall spread of stimulation.

3.5. Sex differences

No statistically significant differences were observed between male and female models in all thresholds of E-Max. Further, there were no statistically significant differences in BSD, although there were statistically significant differences in CSF thickness ($p = 0.04$, t-score = 2.06), with male models having thicker CSF. This difference carried over to V-Half (1 cm^3)

Author Manuscript Author Manuscript Author Manuscript Author Manuscript

where it was observed that male models received less focal and more diffuse stimulation than female models ($p = 0.03$, t-score = 2.31). It has been previously reported that men may have thicker skulls, more intracranial volume, and more CSF volume than females (Gur et al., 2002). Our result that men have a thicker layer of CSF at the vertex corresponds with the observed difference in CSF volume, but no difference was observed in BSD, and the effects on stimulation outcomes (although significant for V-Half 1 cm^3) are likely too small to be considered in TMS studies.

3.6. Effect of coil orientation

The effect of coil orientation on stimulation outcomes over the motor cortex was first described experimentally (Brasil-Neto et al., 1992) and later with biophysical models (Laakso et al., 2014). The effects of coil orientation are likely due to some combination of the fact that there is a preferential coil orientation for the intensity of the induced electric field to be maximized (Laakso et al., 2014; Janssen et al., 2015) and that the direction of the induced intracranial currents in relation to the axis of neurons effects the neurophysiological response to stimulation (Day et al., 1989; Goetz et al., 2016; Hannah and Rothwell, 2016).

Group averaged results of our simulations on 25 models showed an orientation specific response to both E-Max (1 cm^3) and V-Half (1 cm^3) as seen in Fig. 6. A clear parabolic relationship exists between E-Max (1 cm^3) and coil orientation so that when the anterior-posterior axis of the coil is oriented parallel to the longitudinal fissure, stimulation intensities are approximately 90% the intensity as when the coil is oriented perpendicular to the longitudinal fissure. Because 80° and 100° rotations were explored due to the 20° increments used in simulations, it would be expected that our results slightly underestimate the 90° (perpendicular) case. The histogram in Fig. 7 further shows that none of the 25 models had their highest stimulation intensity in the case where the coil was oriented parallel to the longitudinal fissure, but the strongest orientation occurred in over 50% of models between 80° and 100°. Analysis of V-Half (1 cm^3) also highlights an orientation specific relationship, as seen in Fig. 6.

By using manually placed spheres on each model similar to Fig. 2, it is found that the relationship with coil orientation and E-Max may not be representative of all areas being stimulated by TMS. For all three medial spheres, it was observed that stimulation intensities were more commonly maximized when the coil was oriented parallel to the longitudinal fissure and minimized when the coil was oriented perpendicular. This diverges from the overall relationship between both E-Max and coil orientation, and the dorsal seed's E-Field and coil orientation. Specifically, the first seed that is roughly 1.5 cm lateral of the most superior, midline point of the left hemisphere sees E-Field intensities only 59% that of the near perpendicular orientation at the parallel orientation. Differences in the E-Field outcomes between the parallel and perpendicular orientation can be further seen for all seeds in Table 1.

4. Discussion

The results presented in this study use simulations over the vertex on 50 head models of healthy young individuals from the Human Connectome Project database to explore inter-

Author Manuscript Author Manuscript Author Manuscript Author Manuscript

subject variability in TMS effects (i.e. stimulation location, intensity and spread) as a function of non-brain anatomy (i.e. BSD and CSF thickness). In addition, we explore the impact of coil orientation on both the maximum stimulation intensity and the location of maximum stimulation. Our simulations tested different thresholds (1, 10, 100 and 1000 mm^3) to determine the E-Max, V-Half, and A-Half, and concluded that more conservative and less focal thresholds (i.e. 1 cm^3) provided more stable measures. These measures were able to highlight the contributions of both BSD and CSF thickness to stimulation intensity and spread.

Considering the general variability in stimulation location, intensity, and spread, the following observations were made:

- The point of maximum stimulation was within a range of 4 cm in the anterior-posterior direction and 3 cm in the left-right direction of the “hot spot” directly beneath the coil (using spherical seeds).
- Stimulation intensity ranged from 83 to 188 V/m (mean 127, standard deviation 22 V/m) measured through E-Max (1 cm^3).
- Stimulation spread ranged from 6.8 to 24.4 cm^3 (mean 14.9, standard deviation 4.7 cm^3) measured through V-Half (1 cm^3).

In addition to understanding the role of fixed anatomical variables, we tested the impact of coil orientation on intra-subject variability in stimulation intensity and the relative location of stimulation. We describe that placing the coil with the anterior-posterior axis perpendicular to the longitudinal fissure leads to the strongest overall stimulation intensities, while a parallel orientation leads to the weakest intensities (90% as strong). In addition, we describe how the orientation perpendicular to the fissure optimally stimulates the dorsal surface, while the medial wall is preferentially stimulated by parallel orientations.

4.1. Intensity vs. Spread

It is still unknown what the ideal stimulation intensity is for TMS, and that is beyond the scope of this text. Relevant to this work though, once the optimal stimulation intensity is obtained, there will still be a need to choose if stimulation should be scaled according to a desired measure of intensity or to a measure of focality. It is possible to normalize stimulation intensity or stimulation spread, but for a fixed coil at a fixed site of stimulation, it is not possible to adjust both simultaneously. Because of this, if the stimulation intensity is normalized between individuals, some may receive high stimulation intensity in three times as much brain volume as others (using definition of V-Half 1 cm^3). Some adjustments to focality can still be made by altering the coil orientation or the size of the coil that is used, but limitations in the flexibility of scaling will continue to be an impediment to TMS’s accuracy until more complex multi-coil arrays are developed in integrative computational systems (Cline et al., 2015).

4.2. Brain-Scalp distance and cerebrospinal fluid thickness

As would be expected due to the decay of the magnetic field, and in agreement with our previous work (Lee et al., 2016), there is a strong relationship between BSD and maximum

Author Manuscript Author Manuscript Author Manuscript Author Manuscript

stimulation intensity (E-Max). This is a well-known fact that need not be proven in a large modeling study. Using the largest number of head models to date in a TMS study (to the authors' knowledge), our work was able to quantify the impact of BSD on stimulation intensity, and described that 72% of the variability in E-Max (1 cm^3) is explained by BSD. This value is large enough for BSD to be considered a critical predictor of stimulation intensity but also highlights the potential for further predictive precision incorporating detailed finite element models. BSD is also a significant predictor of the spread of stimulation (V-Half and A-Half), with higher BSD resulting in greater spread (or lesser focality).

Similar trends with E-Max and V-Half were also observed with CSF thickness, where thicker layers of CSF contribute to less intense and more diffuse stimulation. Previous modeling studies have also looked into the effects of CSF, highlighting the tendency of high E-Field intensities in grey matter to occur where CSF is thinnest (Bijsterbosch et al., 2012; Janssen et al., 2013). The presented results look not at how CSF thickness relates to the preferential stimulation of certain gyri but instead considers the entire brain. An important difference between our results and previous works is that the effect of CSF was shown independent of BSD. This means that stimulation is not only stronger because individuals with thin CSF also have small BSDs, but because of the specific high conductivity of CSF, discussed in previous theoretical (Miranda et al., 2003) and modeling work (Opitz et al., 2011). Most importantly, a novel finding in our study highlights the influence of CSF not only on stimulation intensity but also on its spread and focality. We demonstrated this with both V-Half and the tendency of individuals with thicker CSF to have the point of maximum stimulation further away from the expected "hot spot" immediately below the coil.

The effects of BSD are not thought to truly be a factor of anatomy per se, but rather a factor of the coil's magnetic field. Because of this, if the coil was placed 3 cm superior to the surface of the brain for all individuals, it would be expected that any relationships between the stimulation profile and BSD would either be greatly diminished or non-existent. The reason why BSD is an important factor is that the coil is not placed at a fixed distance from the brain but instead a fixed distance from the scalp. So, BSD represents a place-holder for how far the coil is from the cortex which is key for understanding the stimulation intensity (because of the magnetic field decay) and spread (because of axial diffusion of the magnetic field further from the coil).

Alternatively, the effects of CSF thickness are thought to be more purely related to the dielectric properties of the fluid. Miranda et al. (Miranda et al., 2003) drew the conclusion using spherical head models, that it was possible for the interface between grey matter and CSF to increase the induced electric field from TMS by a factor up to 1.6. This is due to the disassociation of conductivities between grey matter and CSF, where CSF has greatly increased conductivity (by factor of 19 according to the Foundation for Research on Information Technologies in Society (IT'IS) database (Hasgall et al., 2012), factor of 4 used in Miranda et al. (Miranda et al., 2003)). Accordingly, this disassociation leads to stronger local peaks in stimulation for areas (or individuals) with thinner CSF, effectively amplifying the electric field induced in the brain. Measures of stimulation's relative spread are also expected to be influenced by CSF thickness because thicker layers of CSF reduce the

Author Manuscript Author Manuscript Author Manuscript Author Manuscript

frequency of these strong local maximums directly beneath the coil, thus leading to greater relative spread.

The effects of CSF thickness may be relevant for the use of TMS with elderly populations and conditions with marked cortical atrophy such as Alzheimer's disease and other neurodegenerative dementias, as common morphological symptoms of aging and Alzheimer's include increased cortical CSF volume (Cuingnet et al., 2011; Good et al., 2001). Any increase in cortical CSF volume would be expected to not only to weaken stimulation intensity, but also cause it to be more diffuse in comparison to individuals with less atrophy. This effect may need to be controlled when comparing TMS outcomes in cohorts with wide age spans or between populations in different stages of Alzheimer's disease.

4.3. Orientation specific Effects: Distribution of stimulation

Our results show that (irrespective of location) maximum stimulation intensities occur when the anterior-posterior axis of the coil is oriented perpendicular to the longitudinal fissure, just as maximum stimulation intensities over the hand-motor area occur when the coil is oriented perpendicular to the precentral gyrus (Laakso et al., 2014; Brasil-Neto et al., 1992). We see roughly 10% stronger stimulation intensities (E-Max 1 cm^3) when the coil is oriented perpendicularly in comparison with the parallel orientation. This is also in agreement with previous simulations from Janssen et al. with the coil placed over the supplementary motor area (Janssen et al., 2015). Interestingly though, these results are specific for the dorsal bank of the fissure, while the medial bank showed preference for stimulation at the parallel orientation.

This highlights that the optimal coil orientation for stimulating midline structures depends on the location of the specific target. Without considering the effects of induced current direction on stimulation efficacy, the obvious choice for stimulating more dorsal structures would include a coil orientation perpendicular to the longitudinal fissure. For medial targets, this would seem to change to an orientation parallel to the longitudinal fissure. If both medial and dorsal areas are of interest, then the perpendicular orientation may perform better because the decrease in stimulation intensities in medial structures for the perpendicular orientation is much less than the decrease in stimulation for the parallel case for dorsal structures. Alternatively, since the dorsal surface receives higher stimulation intensities than the medial surface, a parallel orientation could also be considered and stimulation employed at a higher intensity so that the dorsal and medial surface receive more similar stimulation intensities. Finally, as both the dorsal and two most superior medial seeds have approximately symmetrical relationships between coil orientation and E-Field intensity, these results can similarly be applied to either hemisphere, as in the case of bilateral stimulation.

These assessments are solely based on the magnitude of the electric field, and pay no respect to the directional component of the induced fields with respect to gyral surfaces (and neuronal axons). There is expected to be some effect of current direction on stimulation outcome, which is clearly shown from direct stimulation of nerves (Rushton, 1927), and has been hypothesized to effect TMS in the cortical column cosine model (Fox et al., 2004), but

Author Manuscript Author Manuscript Author Manuscript Author Manuscript

the predictive value of the normal component of the electric field has been limited in detailed TMS studies (Bungert et al., 2016).

4.4. Orientation specific Effects: Discussion with neurophysiology

Interestingly, the optimal coil orientation for lower-limb motor thresholds (where the coil is commonly placed over the vertex (Sakai et al., 1994; Nielsen et al., 1995)), is near the perpendicular orientation (i.e. lateral current flow) (Rossini et al., 2015; Sakai et al., 1994; Richter et al., 2013). Because the area between the dorsal and medial surface of the precentral gyrus is known to house knee motor neurons (Penfield and Jasper, 1954) and the medial surface known to house motor neurons of the ankle and foot (Allison et al., 1996; Penfield and Jasper, 1954), it could be expected that the optimal orientation for stimulating these units would be the optimal direction for maximizing the induced electric field in the two most superior medial seeds. Alternatively, we see that the electric field is minimized at the orientation that produces the greatest neurophysiological response. There are two likely possibilities for why this discrepancy occurs. The first possibility is that the perpendicular coil orientation maximizes stimulation effects through providing a more optimal current direction. Because currents will flow perpendicular to the medial crown of the precentral gyrus, neurons could have increased stimulation effects, even though the electric field is weaker in magnitude (in accordance with model from Fox et al. (Fox et al., 2004)). The second likely possibility is that stimulation effects are not initiated at the medial crown, but instead at the dorsal surface where the electric field is maximized during the perpendicular orientation.

Although the surface represented by our dorsal seed (see Fig. 2) is more lateral than the conventionally described source of lower-limb motor neurons, invasive electrical stimulation from researchers including Penfield has clearly shown lower-limb response in the dorsal portion of the precentral gyrus (Woolsey et al., 1979; Penfield and Boldrey, 1937; Wood et al., 1988). This illustrates that it should at least be possible for this area to initiate a motor response in the lower extremity, and this seems to be further supported by some of the dorsal sites of stimulation identified in neuronavigated lower-limb assessments with TMS (Niskanen et al., 2010). Similarly likely though, is the alternative option that the most superior medial area is being preferentially activated by the orientation that is thought to have the optimal neuronal response. This orientation has E-Field intensities only 8% below the parallel case, such that any improvement in neuronal effects because of the direction of current flow would only have to be small to overcome the weaker electric field intensity. These two mechanisms are not mutually exclusive, and it is possible that both magnitude effects on the dorsal surface and directional effects on the medial surface contribute to generating a lower threshold motor evoked potential.

Considering which medial seeds contribute to lower-limb potentials, it seems evident that the more inferior medial seeds are less likely to be directly stimulated by TMS with standard figure-8 coils. The most inferior medial seed in our study has an E-Field intensity 24% of the most superior, and the second most inferior seed has an E-Field intensity still only 51% that of its superior (at optimal orientation for each). Thus, stimulation delivered to the lower medial seeds would need to be conducted while providing roughly 2 to 4 times the

Author Manuscript Author Manuscript Author Manuscript Author Manuscript

stimulation intensity to both the superior medial and dorsal seed. Also, the orientation dependent effects seen in the middle medial seed are greater than those seen in the most superior seed, so that any advantages of the perpendicular orientation from current direction would need to overcome a 15% deficit in magnitude (as opposed to 8%), further amplifying the stimulation differences of inferior medial areas.

Finally, although this section has considered orientations in the idealized absolutes of either the perpendicular or parallel orientation case, it is worthwhile to remember that not all individuals have the same relationship between coil orientation and stimulation intensity. A significant portion of subjects do not follow the group average trend. This heterogeneity can be supported by previous recordings of lower-limb motor neuron activity by Di Lizzaro et al., which has shown specific individuals to have both much greater motor thresholds for the parallel orientation (145% perpendicular case) and much greater thresholds for the perpendicular orientation (127% the parallel case) (Di Lazzaro et al., 2001) (similar dissociations seen in Richter et al. (Richter et al., 2013)), highlighting that although these group trends are important, they are not a hard rule for all subjects.

4.5. Limitations

A technical limitation of the orientation dependent conclusion stated here is that our results do not take anisotropic conductivities or fiber tracts into account. Although the majority of measures used in this study are likely only affected in a limited way by anisotropic conductivities, future studies could test if more detailed models give support to an alternative hypothesis of the mechanisms of TMS induced lower-limb activation. Further, although the coil position of the vertex is commonly used for lower-limb motor assessments (Sakai et al., 1994; Priori et al., 1993), the spherical regions of interest placed in each subject were not necessarily localized in the precentral gyrus. The authors do not have any reason to believe that this would have any effect on simulation results or the conclusions drawn.

Finally, even though our head models represent complex brain geometry, additional anatomical regions could be segmented for further confirmation of results. The main anatomical component of interest for simulations over midline would be the falx cerebri, a layer of dura roughly 2 mm thick that separates the two hemispheres of the brain (Miga et al., 1999). This area is difficult to segment and thus is not even included in the high resolution MIDA head model (Iacono et al., 2015), although it has been modeled as a discontinuous medium in some studies (Laakso et al., 2016b).

5. Conclusion

Our results highlight the distinct role of both BSD and CSF thickness in shaping the site of stimulation. Still, because of the large number of anatomical factors that are related to stimulation and the degree of variance left unexplained by gross non-brain factors, finite element simulations are well suited to quantify differences in the induced E-Field from TMS. Moving beyond biophysics, factors such as state-dependent features (Luber et al., 2017; Siebner et al., 2009) and functional organization (Drysdale et al., 2017; Rosso et al., 2017; Wang et al., 2015) will also affect stimulation outcomes. Although these biological variables unrelated to current modeling efforts will affect stimulation effects, understanding

Author Manuscript Author Manuscript Author Manuscript Author Manuscript

how the site of stimulation differs between individuals is an important step to understand biological contributors to inter-subject variability.

The inter-subject variability and relationships observed in our simulations may best be applied to cases of stimulation over bilateral midline targets. Specific factors such as overall brain curvature, the presence of the longitudinal fissure, and thick CSF layers, make the vertex relatively dissimilar to targets such as the hand-motor knob or the dorsolateral prefrontal cortex. The previously mentioned anatomical factors are most similar to the vertex at the portion of the brain for the next several centimeters anterior of the vertex, covering targets such as the somatosensory cortex, primary motor cortex, supplementary motor area, and dorsomedial prefrontal cortex. Because of this, the ranges of variability outlined here are best interpreted under the context of midline targets. Although it is expected that similar relationships hold with BSD and CSF thickness over other regions of the brain, the range of both BSD and CSF thickness may differ depending on the target area. Further, it is expected that the vertex may have rather high inter-subject variability, but other elements of our study including age, health status, and conductivities estimates were all likely to reduce inter-subject variability.

Researchers interested in using a further refined version of the models used in this study for their own work can download the models in a variety of formats through the IT'IS website at http://www.itis.ethz.ch/virtual-population/regional-human-models/phmrepository/.

Supplementary Material

Refer to Web version on PubMed Central for supplementary material.

Acknowledgements

This work was sponsored by the Carver Charitable Trust and the Palmer Endowment Fund. Data were provided [in part] by the Human Connectome Project, WU-Minn Consortium (Principal Investigators: David Van Essen and Kamil Ugurbil; 1U54MH091657) funded by the 16 NIH Institutes and Centers that support the NIH Blueprint for Neuroscience Research; and by the McDonnell Center for Systems Neuroscience at Washington University.

Glossary

E-Max	The maximum electric field intensity in the brain.
V-Half	The volume of the brain stimulated at an E-Field intensity at least half of E-Max for a given simulation.

References

Allison T, McCarthy G, Luby M, Puce A, Spencer DD. Localization of functional regions of human mesial cortex by somatosensory evoked potential recording and by cortical stimulation. Electroencephalogr Clin Neurophysiol 1996;100:126–40. 10.1016/0013-4694(95)00226-X. [PubMed: 8617151]

Barker AT, Jalinous R, Freeston IL. Non-invasive magnetic stimulation of human motor cortex. Lancet 1985;1:1106–7. 10.1016/S0140-6736(85)92413-4. [PubMed: 2860322]

Berlim MT, van den Eynde F, Tovar-Perdomo S, Daskalakis ZJ. Response, remission and drop-out rates following high-frequency repetitive transcranial magnetic stimulation (rTMS) for treating

Author Manuscript Author Manuscript Author Manuscript Author Manuscript

major depression: a systematic review and meta-analysis of randomized, double-blind and sham-controlled trials. Psychol Med 2014;44:225–39. 10.1017/S0033291713000512. [PubMed: 23507264]

Bijsterbosch JD, Barker AT, Lee KH, Woodruff PWR. Where does transcranial magnetic stimulation (TMS) stimulate? Modelling of induced field maps for some common cortical and cerebellar targets. Med Biol Eng Comput 2012;50:671–81. 10.1007/s11517-012-0922-8. [PubMed: 22678596]

Brasil-Neto JP, Cohen LG, Panizza M, Nilsson J, Roth BJ, Hallett M. Optimal focal transcranial magnetic activation of the human motor cortex: effects of coil orientation, shape of the induced current pulse, and stimulus intensity. J Clin Neurophysiol 1992;9:132–6. 10.1097/00004691-199201000-00014. [PubMed: 1552001]

Bungert A, Antunes A, Espenhahn S, Thielscher A. Where does TMS stimulate the motor cortex? Combining electrophysiological measurements and realistic field estimates to reveal the affected cortex position. Cereb Cortex 2016:1–12. 10.1093/cercor/bhw292. [PubMed: 25139941]

Chieffo R, De Prezzo S, Houdayer E, Nuara A, Di Maggio G, Coppi E, et al. Deep repetitive transcranial magnetic stimulation with h-coil on lower limb motor function in chronic stroke: a pilot study. Arch Phys Med Rehabil 2014;95:1141–7. 10.1016/j.apmr.2014.02.019. [PubMed: 24625546]

Cline CC, Johnson NN, He B. Subject-specific optimization of channel currents for multichannel transcranial magnetic stimulation. Proc Annu Int Conf IEEE Eng Med Biol Soc EMBS 2015;2015–Novem:2083–6. 10.1109/EMBC.2015.7318798.

Crowther LJ, Hadimani RL, Jiles DC. Effect of Anatomical Brain Development on Induced Electric Fields During Transcranial Magnetic Stimulation. IEEE Trans Magn 2014;50.

Cuingnet R, Gerardin E, Tessieras J, Auzias G, Lehéricy S, Habert MO, et al. Automatic classification of patients with Alzheimer's disease from structural MRI: a comparison of ten methods using the ADNI database. Neuroimage 2011;56:766–81. 10.1016/j.neuroimage.2010.06.013. [PubMed: 20542124]

Cunnington R, Iansek R, Thickbroom GW, Laing BA, Mastaglia FL, Bradshaw JL, et al. Effects of magnetic stimulation over supplementary motor area on movement in Parkinson's disease. Brain 1996;119:815–22. 10.1093/brain/119.3.815 [PubMed: 8673493]

Day BL, Dressler D, de Noordhout AM, Marsden CD, Nakashima K, Rothwell JC, et al. Electric and magnetic stimulation of human motor cortex: surface EMG and single motor unit responses. J Physiol 1989;412:449–73. 10.1113/jphysiol.1989.sp017626. [PubMed: 2489409]

Deng ZD, Lisanby SH, Peterchev AV. Electric field depth-focality tradeoff in transcranial magnetic stimulation: Simulation comparison of 50 coil designs. Brain Stimul 2013;6:1–13. 10.1016/j.brs.2012.02.005. [PubMed: 22483681]

Diedenhofen B, Musch J. Cocor : a comprehensive solution for the statistical comparison of correlations. PLoS One 2015:1–12. 10.1371/journal.pone.0121945.

Downar J, Geraci J, Salomons TV, Dunlop K, Wheeler S, Mcandrews MP, et al. Anhedonia and reward-circuit connectivity distinguish nonresponders from responders to dorsomedial prefrontal repetitive transcranial magnetic stimulation in major depression. Biol Psychiatry 2014;76:176–85. 10.1016/j.biopsych.2013.10.026. [PubMed: 24388670]

Drysdale AT, Grosenick L, Downar J, Dunlop K, Mansouri F, Meng Y, et al. Restingstate connectivity biomarkers define neurophysiological subtypes of depression. Nat Med 2017;23:28–38. 10.1038/nm0217-264d. [PubMed: 27918562]

Van Essen DC, Ugurbil K, Auerbach E, Barch D, Behrens TEJ, Bucholz R, et al. The human connectome project: a data acquisition perspective. Neuroimage 2012;62:2222–31. 10.1016/j.neuroimage.2012.02.018. [PubMed: 22366334]

Fox PT, Narayana S, Tandon N, Sandoval H, Fox SP, Kochunov P, et al. Column-based model of electric field excitation of cerebral cortex. Hum Brain Mapp 2004;22:1–16. 10.1002/hbm.20006. [PubMed: 15083522]

Goetz SM, Luber B, Lisanby SH, Murphy DLK, Kozyrkov IC, Grill WM, et al. Enhancement of Neuromodulation with novel pulse shapes generated by controllable pulse parameter transcranial magnetic stimulation. Brain Stimul 2016;9:39–47. 10.1016/j.brs.2015.08.013. [PubMed: 26460199]

Author Manuscript Author Manuscript Author Manuscript Author Manuscript

Good CD, Johnsrude IS, Ashburner J, Henson RN, Friston KJ, Frackowiak RS. A voxel-based morphometric study of ageing in 465 normal adult human brains. Neuroimage 2001;14:21–36. 10.1006/nimg.2001.0786. [PubMed: 11525331]

Grunhaus L, Schreiber S, Dolberg OT, Polak D, Dannon PN. A randomized controlled comparison of electroconvulsive therapy and repetitive transcranial magnetic stimulation in severe and resistant nonpsychotic major depression. Biol Psychiatry 2003;53:324–31. 10.1016/S0006-3223(02)01499-3. [PubMed: 12586451]

Gur RC, Ginning-Dixon F, Bilker WB, Gur RE. Sex differences in temporo-limbic and frontal brain volumes of healthy adults. Cereb Cortex 2002;12:998–1003. 10.1093/cercor/12.9.998. [PubMed: 12183399]

Hannah R, Rothwell JC. Pulse duration as well as current direction determines the specificity of transcranial magnetic stimulation of motor cortex during contraction. Brain Stimul 2016;10:106–15. 10.1016/j.brs.2016.09.008. [PubMed: 28029595]

Hasgall PA, Neufeld E, Gosselin MC, Klingenböck A, Kuster N. IT'IS database for thermal and electromagnetic parameters of biological tissues, version 2.2. July 11th 2012.

Hovey C, Jalinous R. The Guide To Magnetic Stimulation. Whitland, Wales: Magstim; 2006.

Iacono MI, Neufeld E, Akinnagbe E, Bower K, Wolf J, Oikonomidis IV, et al. MIDA: A multimodal imaging-based detailed anatomical model of the human head and neck. PLoS One 2015;10 10.1371/journal.pone.0124126.

Janssen AM, Oostendorp TF, Stegeman DF. The coil orientation dependency of the electric field induced by TMS for M1 and other brain areas. J Neuroeng Rehabil 2015;12:47 10.1186/s12984-015-0036-2. [PubMed: 25981522]

Janssen AM, Rampersad S, Lucka F, Lanfer B, Lew S, Aydin U, et al. The influence of sulcus width on simulated electric fields induced by transcranial magnetic stimulation. Phys Med Biol 2013;58:4881–96. 10.1088/00319155/58/14/4881. [PubMed: 23787706]

Kakuda W, Abo M, Watanabe S, Momosaki R, Hashimoto G, Nakayama Y, et al. High-frequency rTMS applied over bilateral leg motor areas combined with mobility training for gait disturbance after stroke: a preliminary study. Brain Inj 2013;27:1080–6. 10.3109/02699052.2013.794973. [PubMed: 23834634]

Kennerley SW. Organization of Action Sequences and the Role of the Pre-SMA. J Neurophysiol 2003;91:978–93. 10.1152/jn.00651.2003. [PubMed: 14573560]

Kleim JA, Chan S, Pringle E, Schallert K, Procaccio V, Jimenez R, et al. BDNF val66met polymorphism is associated with modified experience-dependent plasticity in human motor cortex. Nat Neurosci 2006;9:735–7. [PubMed: 16680163]

Krieg TD, Salinas FS, Narayana S, Fox PT, Mogul DJ. Computational and experimental analysis of TMS-induced electric field vectors critical to neuronal activation. J Neural Eng 2015;12:46014 10.1088/1741-2560/12/4/046014.

Laakso Ilkka; Murakamo T Thresholds of Central Nervous System Stimulation at Intermediate Frequencies. 2016 URSI Asia-Pacific Radio Sci Conf August 2016a:733–6.

Laakso I, Hirata A. Reducing the staircasing error in computational dosimetry of low-frequency electromagnetic fields. Phys Med Biol 2012;57:25–34. 10.1088/0031-9155/57/4/N25.

Laakso I, Hirata A, Ugawa Y. Effects of coil orientation on the electric field induced by TMS over the hand motor area. Phys Med Biol 2014;59:203–18. 10.1088/0031-9155/59/1/203. [PubMed: 24334481]

Laakso I, Tanaka S, Mikkonen M, Koyama S, Sadato N, Hirata A. Electric fields of motor and frontal tDCS in a standard brain space: A computer simulation study. Neuroimage 2016b;137:140–51. 10.1016/j.neuroimage.2016.05.032. [PubMed: 27188218]

Di Lazzaro V, Oliviero A, Profice P, Meglio M, Cioni B, Tonali P, et al. Descending spinal cord volleys evoked by transcranial magnetic and electrical stimulation of the motor cortex leg area in conscious humans. J Physiol 2001;537:1047–58. [PubMed: 11744776]

Lee EG, Duffy W, Hadimani RL, Waris M, Siddiqui W, Islam F, et al. Investigational effect of brain-scalp distance on the efficacy of transcranial magnetic stimulation treatment in depression. IEEE Trans Magn 2016;52:52–5. 10.1109/TMAG.2015.2514158.

Author Manuscript Author Manuscript Author Manuscript Author Manuscript

Luber BM, Davis S, Bernhardt E, Neacsiu A, Kwapil L, Lisanby SH, et al. Using neuroimaging to individualize TMS treatment for depression: toward a new paradigm for imaging-guided intervention. Neuroimage 2017 10.1016/j.neuroimage.2016.12.083.

Maeda F, Keenan JP, Tormos JM, Topka H, Pascual-Leone A. Modulation of corticospinal excitability by repetitive transcranial magnetic stimulation. Clin Neurophysiol 2000;111:800–5. 10.1016/S1388-2457(99)00323-5. [PubMed: 10802449]

Mantovani A, Westin G, Hirsch J, Lisanby SH. Functional magnetic resonance imaging guided transcranial magnetic stimulation in obsessive-compulsive disorder. Biol Psychiatry 2010;67:e39–40. 10.1016/j.biopsych.2009.08.009. [PubMed: 19793582]

Miga MI, Paulsen KD, Kennedy FE, Hartov A, Roberts DW. Model-Updated Image-Guided Neurosurgery Using the Finite Element Method: Incorporation of the Falx Cerebri. Med Image Comput Comput Assist Interv 1999:900–10. [PubMed: 26317119]

Miranda PC, Hallett M, Basser PJ. The electric field induced in the brain by magnetic stimulation: A 3-D finite-element analysis of the effect of tissue heterogeneity and anisotropy. IEEE Trans Biomed Eng 2003;50:1074–85. 10.1109/TBME.2003.816079. [PubMed: 12943275]

Nielsen J, Petersen N, Ballegaard M. Latency of effects evoked by electrical and magnetic brain stimulation in lower limb motoneurones in man. J Physiol 1995;484 (Pt 3:791–802. 10.1113/jphysiol.1995.sp020704. [PubMed: 7623293]

Niskanen E, Julkunen P, Säisänen L, Vanninen R, Karjalainen P, Könönen M. Grouplevel variations in motor representation areas of thenar and anterior tibial muscles: Navigated transcranial magnetic stimulation study. Hum Brain Mapp 2010;31:1272–80. 10.1002/hbm.20942. [PubMed: 20082330]

Obeso I, Robles N, Marron EM, Redolar-Ripoll D. Dissociating the Role of the preSMA in response inhibition and switching: a combined online and offline TMS Approach. Front Hum Neurosci 2013;7:150 10.3389/fnhum.2013.00150. [PubMed: 23616761]

Oliveri M, Babiloni C, Filippi MM, Caltagirone C, Babiloni F, Cicinelli P, et al. Influence of the supplementary motor area on primary motor cortex excitability during movements triggered by neutral or emotionally unpleasant visual cues. Exp Brain Res 2003;149:214–21. 10.1007/s00221-002-1346-8. [PubMed: 12610690]

Opitz A, Fox MD, Craddock RC, Colcombe S, Milham MP. An integrated framework for targeting functional networks via transcranial magnetic stimulation. Neuroimage 2016;127:86–96. 10.1016/j.neuroimage.2015.11.040. [PubMed: 26608241]

Opitz A, Legon W, Rowlands A, Bickel WK, Paulus W, Tyler WJ. Physiological observations validate finite element models for estimating subject-specific electric field distributions induced by transcranial magnetic stimulation of the human motor cortex. Neuroimage 2013;81:253–364. 10.1016/j.neuroimage.2013.04.067. [PubMed: 23644000]

Opitz A, Windhoff M, Heidemann RM, Turner R, Thielscher A. How the brain tissue shapes the electric field induced by transcranial magnetic stimulation. Neuroimage 2011;58:849–59. 10.1016/j.neuroimage.2011.06.069. [PubMed: 21749927]

Pascual-Leone A, Valls-Solé J, Wassermann EM, Hallett M. Responses to rapid-rate transcranial magnetic stimulation of the human motor cortex. Brain 1994;117:847–58. 10.1093/brain/117.4.847. [PubMed: 7922470]

Penfield W, Boldrey E. Somatic motor and sensory representation in man. Brain 1937:389–443. 10.1093/brain/60.4.389.

Penfield W, Jasper H. Epilepsy and the functional anatomy of the human brain. Oxford, England: Little, Brown & Co.; 1954.

Priori A, Bertolasi L, Dressler D, Rothwell JC, Day BL, Thompson PD, et al. Transcranial electric and magnetic stimulation of the leg area of the human motor cortex: single motor unit and surface EMG responses in the tibialis anterior muscle. Electroencephalogr Clin Neurophysiol 1993;89:131–7. [PubMed: 7683603]

Pulvermuller F, Hauk O, Nikulin VV, Ilmoniemi RJ. Functional links between motor and language systems. Eur J Neurosci 2005;21:793–7. 10.1111/j.1460-9568.2005.03900.x. [PubMed: 15733097]

Rastogi P, Lee EG, Hadimani RL, Jiles DC. Transcranial Magnetic Stimulation-coil design with improved focality. AIP Adv 2017;7:56705 10.1063/1.4973604.

Author Manuscript Author Manuscript Author Manuscript Author Manuscript

Richter L, Neumann G, Oung S, Schweikard A, Trillenberg P. Optimal coil orientation for transcranial magnetic stimulation. PLoS One 2013;8:1–10. 10.1371/journal.pone.0060358.

Rochas V, Gelmini L, Krolak-Salmon P, Poulet E, Saoud M, Brunelin J, et al. Disrupting pre-SMA activity impairs facial happiness recognition: an event-related TMS study. Cereb Cortex 2013;23:1517–25. 10.1093/cercor/bhs133. [PubMed: 22661410]

Rossini PM, Burke D, Chen R, Cohen LG, Daskalakis Z, Di Iorio R, et al. Non-invasive electrical and magnetic stimulation of the brain, spinal cord, roots and peripheral nerves: basic principles and procedures for routine clinical and research application. An updated report from an I.F.C.N. Committee. Clin Neurophysiol 2015;126:1071–107. 10.1016/j.clinph.2015.02.001. [PubMed: 25797650]

Rosso C, Perlbarg V, Valabregue R, Obadia M, Kemlin-Méchin C, Moulton E, et al. Anatomical and functional correlates of cortical motor threshold of the dominant hand. Brain Stimul 2017;10:952–8. 10.1016/j.brs.2017.05.005. [PubMed: 28551318]

Rushton WAH. The effect uponn the threshold for nervous excitation of the length of nerve exposed, and the angle between current and nerve. J Physiol 1927;63:357–77. [PubMed: 16993895]

Sakai Y, Kanazawa I, Sakai UK. Transcranial stimulation of the leg area of the motor cortex in humans. Acta Neurol Scand 1994;89:378–83. [PubMed: 8085437]

Salomons TV, Dunlop K, Kennedy SH, Flint A, Geraci J, Giacobbe P, et al. Resting-state cortico-thalamic-striatal connectivity predicts response to dorsomedial prefrontal rTMS in major depressive disorder. Neuropsychopharmacology 2013;39:488–98. 10.1038/npp.2013.222. [PubMed: 24150516]

SEMCAD X S. Partner Engineering AG (SPEAG), version 14.8 Aletsch 2014.

Siebner HR, Hartwigsen G, Kassuba T, Rothwell JC. How does transcranial magnetic stimulation modify neuronal activity in the brain? Implications for studies of cognition. Cortex 2009;45:1035–42. 10.1016/j.cortex.2009.02.007. [PubMed: 19371866]

Stokes MG, Barker AT, Dervinis M, Verbruggen F, Maizey L, Adams RC, et al. Biophysical determinants of transcranial magnetic stimulation: Effects of excitability and depth of targeted area. J Neurophysiol 2013;109:437–44. 10.1152/jn.00510.2012. [PubMed: 23114213]

Thielscher A, Antunes A, Saturnino GB. Field modeling for transcranial magnetic stimulation: A useful tool to understand the physiological effects of TMS? Conf Proc IEEE Eng Med Biol Soc 2015;2015:222–5. 10.1109/EMBC.2015.7318340. [PubMed: 26736240]

Thielscher A, Kammer T. Electric field properties of two commercial figure-8 coils in TMS: calculation of focality and efficiency. Clin Neurophysiol 2004;115:1697–708. 10.1016/j.clinph.2004.02.019. [PubMed: 15203072]

Thielscher A, Opitz A, Windhoff M. Impact of the gyral geometry on the electric field induced by transcranial magnetic stimulation. Neuroimage 2011;54:234–43. 10.1016/j.neuroimage.2010.07.061. [PubMed: 20682353]

Verwey WB, Lammens R, van Honk J. On the role of the SMA in the discrete sequence production task: a TMS study Transcranial magnetic stimulation. Neuropsychologia 2002;40:1268–76. 10.1016/S0028-3932(01)00221-4. [PubMed: 11931929]

Walsh V, Cowey A. Transcranial magnetic stimulation and cognitive neuroscience. Nat Rev Neurosci 2000;1:73–80. [PubMed: 11252771]

Wang D, Buckner RL, Fox MD, Holt DJ, Holmes AJ, Stoecklein S, et al. Parcellating cortical functional networks in individuals. Nat Neurosci 2015;18:1853–60. 10.1038/nn.4164. [PubMed: 26551545]

Williams EJ. The Comparison of Regression Variables. J R Stat Soc Ser B 1959;21:396–9.

Windhoff M, Opitz A, Thielscher A. Electric field calculations in brain stimulation based on finite elements: an optimized processing pipeline for the generation and usage of accurate individual head models. Hum Brain Mapp 2013;34:923–35. 10.1002/hbm.21479. [PubMed: 22109746]

Wood CC, Spencer DD, Allison T, McCarthy G, Williamson PD, Goff WR. Localization of human sensorimotor cortex during surgery by cortical surface recording of somatosensory evoked potentials. J Neurosurg 1988;68:99–111. 10.3171/jns.1988.68.1.0099. [PubMed: 3275756]

Woolsey CNCCN, Erickson TCTTC, Gilson WEWWE. Localization in somatic sensory and motor areas of human cerebral cortex as determined by direct recording of evoked potentials and

Author Manuscript Author Manuscript Author Manuscript Author Manuscript

electrical stimulation. J Neurosurg 1979;51:476–506. 10.3171/jns.1979.51.4.0476. [PubMed: 479934]

Zangen A, Roth Y, Voller B, Hallett M. Transcranial magnetic stimulation of deep brain regions: Evidence for efficacy of the H-Coil. Clin Neurophysiol 2005;116:775–9. 10.1016/j.clinph.2004.11.008. [PubMed: 15792886]

Author Manuscript Author Manuscript Author Manuscript Author Manuscript

HIGHLIGHTS

- Inter-subject variability of TMS effects is driven by normal variation in non-brain anatomy.
- Brain-scalp distance and CSF thickness both affect stimulation intensity and spread.
- The dorsal and medial surfaces of the brain are affected differently by TMS coil orientation.

Author Manuscript Author Manuscript Author Manuscript Author Manuscript

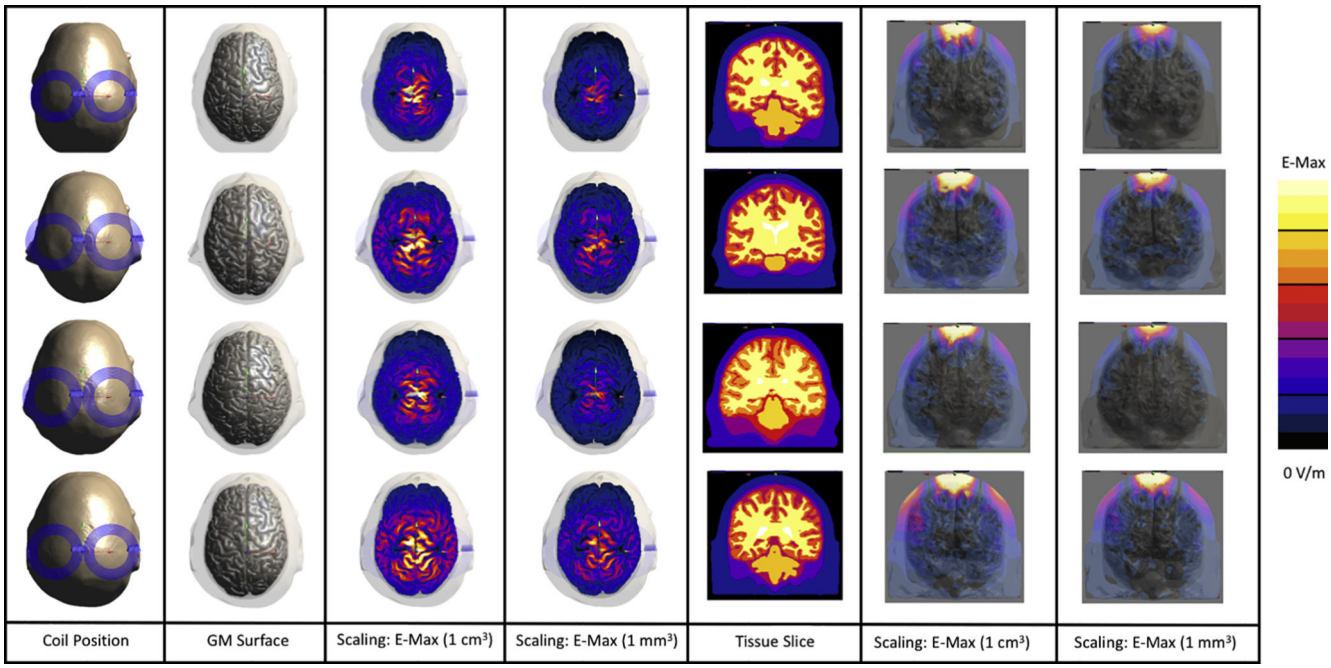

Fig. 1.

Example plot of the anatomy and E-Field distribution for four subjects. From left to right, the columns include the coil position over the vertex, a view of the grey matter surface, a plot of the E-Field on the grey matter surface scaled to E-Max (1 cm^3), a plot of the E-Field on the grey matter surface scaled to E-Max (1 mm^3), a coronal slice highlighting the anatomical distribution at the slice directly below the coil, the induced E-Field at the same slice using E-Max (1 cm^3) for scaling, and a plot using E-Max (1 mm^3) for scaling.

Author Manuscript Author Manuscript Author Manuscript Author Manuscript

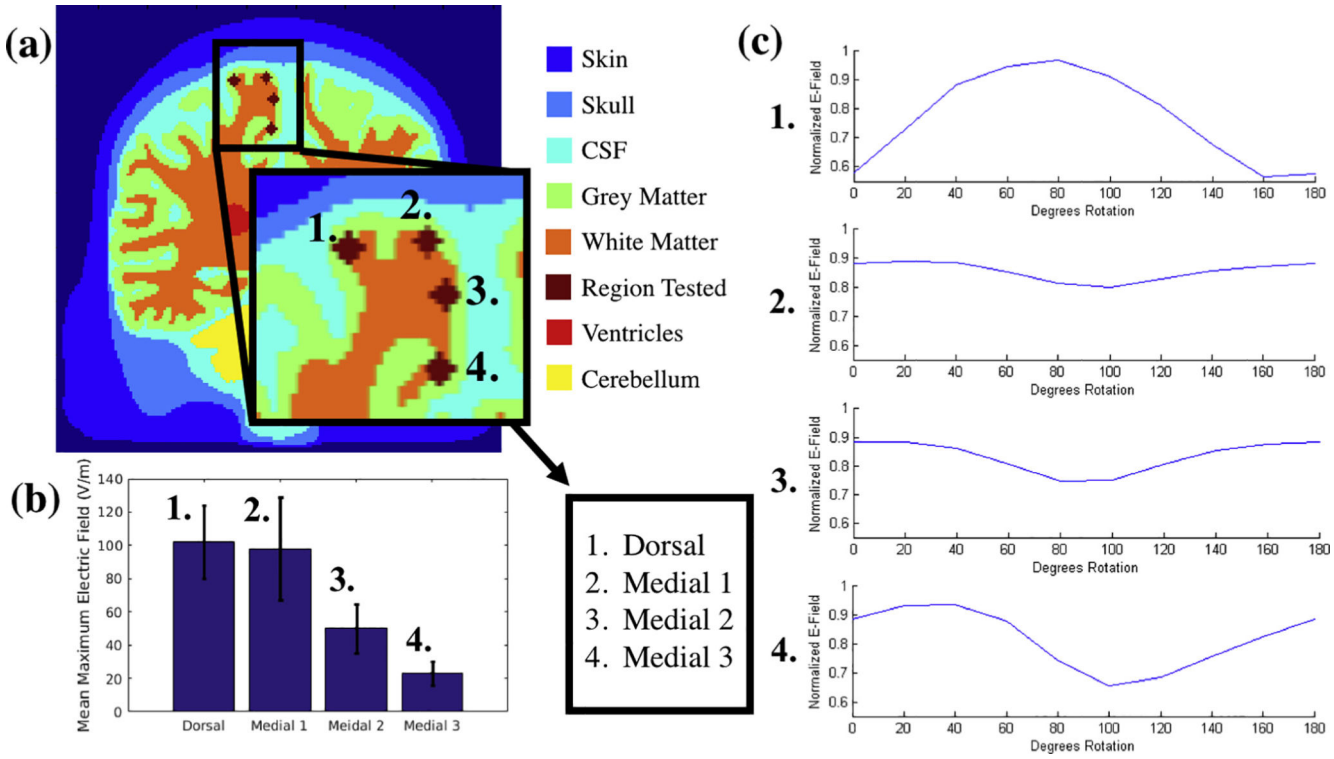

Fig. 2.

(a) Example placement of the four spherical seeds placed on one model. (b) The mean E-Field intensity observed in each of the four spheres for the orientation that yielded the greatest E-Field intensities on a per-subject basis, with the standard deviation represented by error bars. (c) The average E-Field intensity during coil rotations for the 25 models for each seed, normalized to the values from (b).

Author Manuscript Author Manuscript Author Manuscript Author Manuscript

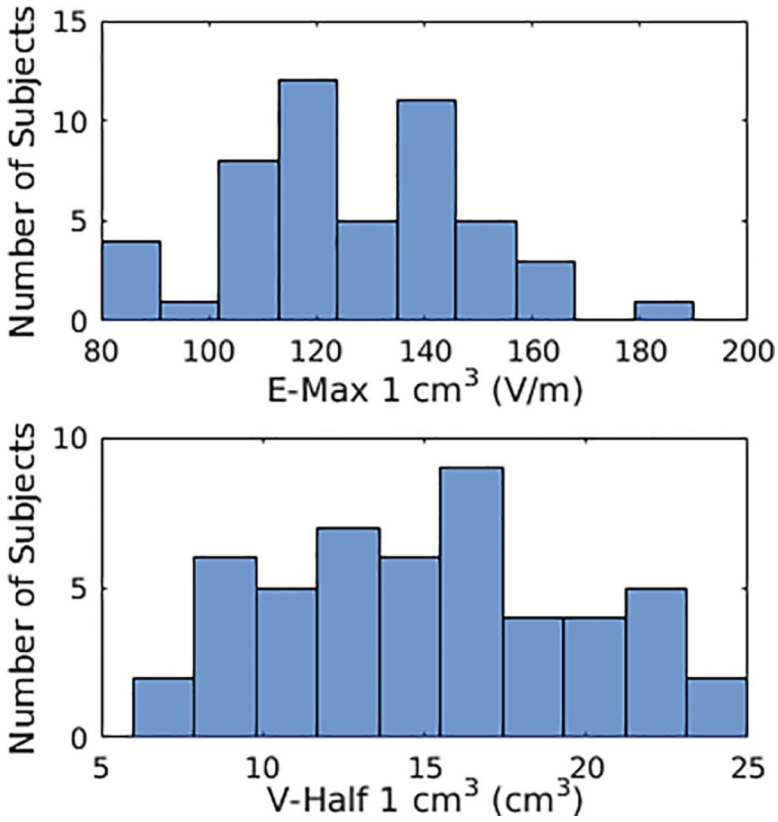

Fig. 3.

In the top plot, the distribution of E-Max (1 cm^3) across all 50 models is shown. In the bottom plot, the distribution of V-Half (1 cm^3) across all 50 models is shown.

Author Manuscript Author Manuscript Author Manuscript Author Manuscript

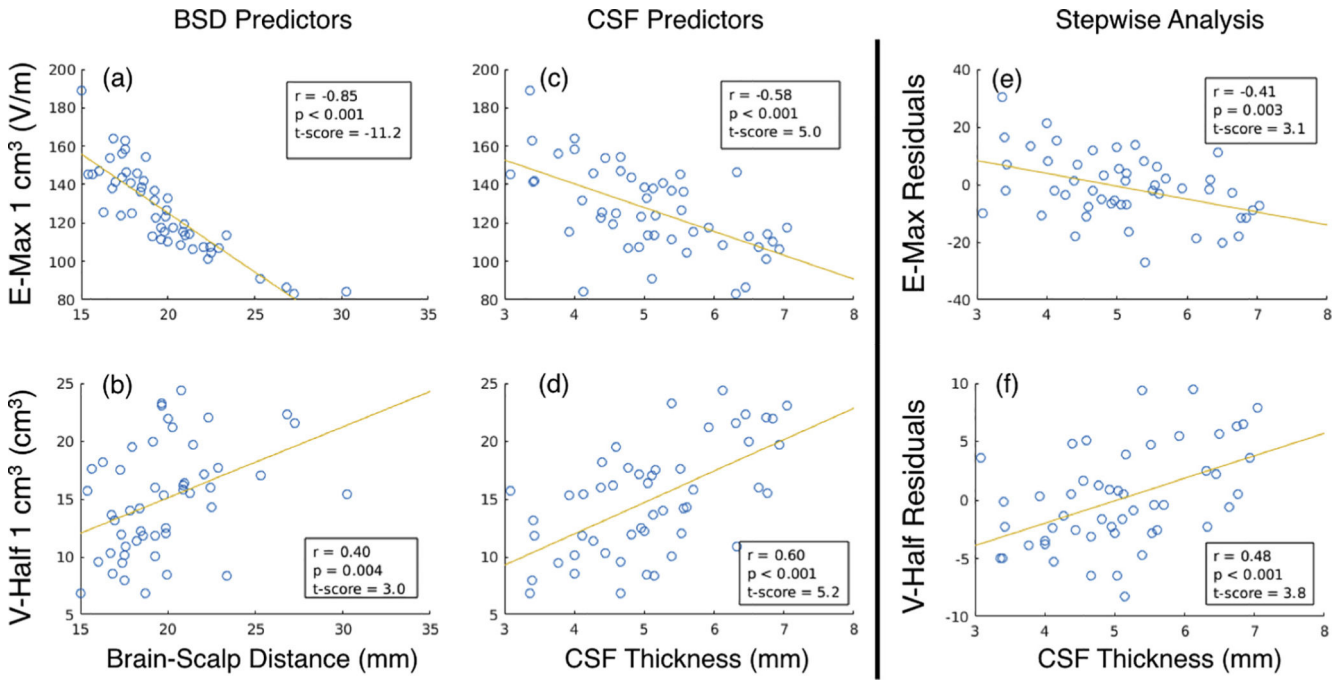

Fig. 4.

(a) Shows the relationship between E-Max (1 cm^3) and brain-scalp distance, including one point for each of the fifty models. (b) Shows the relationship between V-Half (1 cm^3) and brain-scalp distance. Plots (c and d) are equivelant to plots (a and b), only relationships are tested against CSF thickness instead of brain-scalp distance. Plots (e and f) show how CSF predicts the residuals of both E-Max (1 cm^3) and V-Half (1 cm^3) after the effects of brain-scalp distance have been regressed.

Author Manuscript Author Manuscript Author Manuscript Author Manuscript

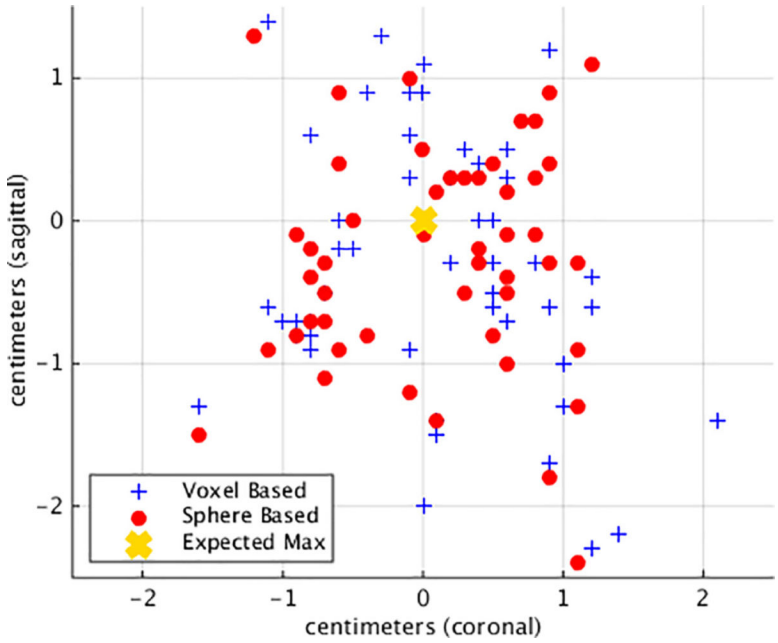

Fig. 5.

View of where the maximum stimulation intensities occur in an axial plane. The x-axis represents distance in the coronal plane and the y-axis represents distance in the sagittal plane. The expected “hot spot” of stimulation is shown at (0,0). The blue crosses represent the location of the voxel with the maximum electric field intensity in the brain. The red spheres represent the location of a similar metric defined by spherical seeds as described in the Methods section.

Author Manuscript Author Manuscript Author Manuscript Author Manuscript

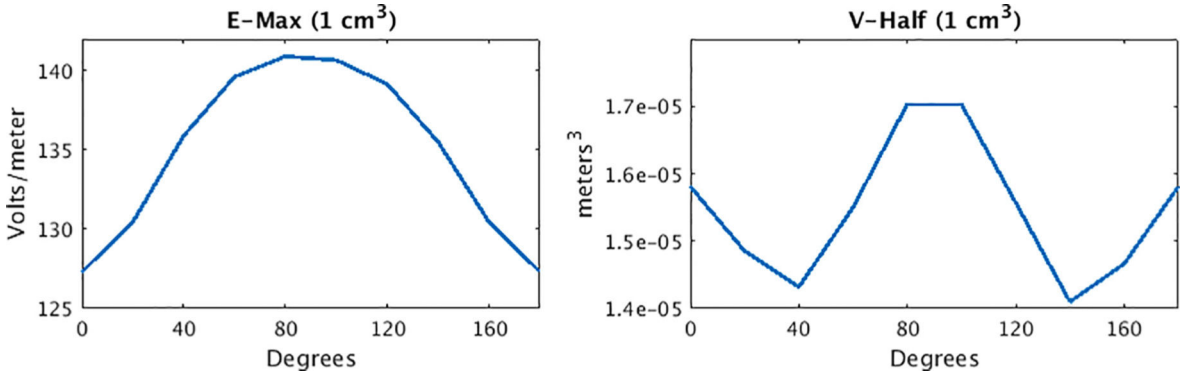

Fig. 6.

Plots showing the group average E-Max (1 cm^3, left) and V-Half (1 cm^3, right), with respect to coil orientation. 0° and 180° represent the case where the coil is oriented parallel to the longitudinal fissure and 90° where the coil is oriented perpendicular to the longitudinal fissure.

Author Manuscript Author Manuscript Author Manuscript Author Manuscript

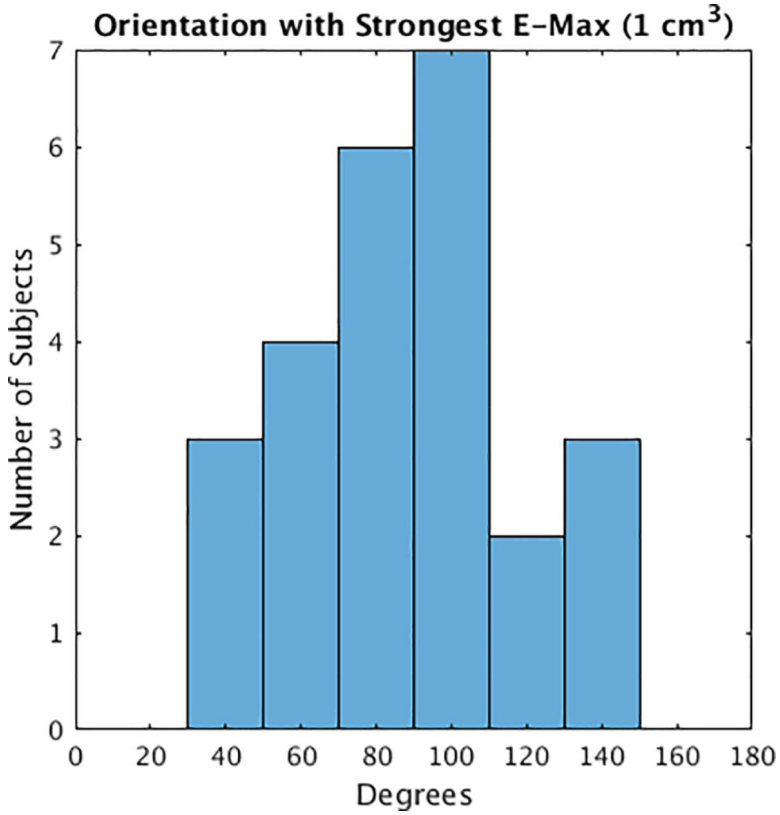

Fig. 7.

Histogram outlining the coil orientation in which models have the orientation that has the strongest E-Max (1 cm^3) value. 0° and 180° represent the case where the coil is oriented parallel to the longitudinal fissue and 90° where the coil is oriented perpendicular to the longitudinal fissure. Results highlight that the strongest stimulation intensities occur most commonly over orientations perpendicular to the longitudinal fissure.

Author Manuscript Author Manuscript Author Manuscript Author Manuscript

Table 1

In first row, statistics are reported for the subject specific optimal orientation (individualized for each seed). These values were used to normalize the E-Field intensity within subjects and within seeds for the next two rows, which describe the normalized E-Field for the parallel and near perpendicular (80° case) in the four seeds shown in Fig. 2.

Measure	Dorsal	Medial 1	Medial 2	Medial 3
E-Field of Greatest Orientation (Mean (SD) in V/m, Used for Normalization)	102 (22)	98 (31)	50 (15)	23 (7)
Normalized E-Field in Parallel Orientation (Mean (SD))	0.57 (0.19)	0.88 (0.13)	0.88 (0.15)	0.89 (0.14)
Normalized E-Field in Near Perpendicular Orientation (i.e. 80°, Mean (SD))	0.97 (0.05)	0.81 (0.18)	0.75 (0.21)	0.74 (0.19)

Clin Neurophysiol. Author manuscript; available in PMC 2019 June 13.